Endothelial focal adhesion kinase mediates cancer cell homing to discrete regions of the lungs via E-selectin up-regulation

Sachie Hiratsuka[a,1], Shom Goel[a], Walid S. Kamoun[a], Yoshiro Maru[b], Dai Fukumura[a,2], Dan G. Duda[a,2], and Rakesh K. Jain[a,2]

[a]Edwin L. Steele Laboratory for Tumor Biology, Department of Radiation Oncology, Massachusetts General Hospital, Harvard Medical School, Boston, MA 02114; and [b]Department of Pharmacology, Tokyo Women's Medical University, Tokyo 162-8666, Japan

Contributed by Rakesh K. Jain, January 10, 2011 (sent for review October 15, 2010)

Primary tumors secrete factors that alter the microenvironment of distant organs, rendering those organs as fertile soil for subsequent metastatic cancer cell colonization. Although the lungs are exposed to these factors ubiquitously, lung metastases usually develop as a series of discrete lesions. The underlining molecular mechanisms of the formation of these discrete lesions are not understood. Here we show that primary tumors induce formation of discrete foci of vascular hyperpermeability in premetastatic lungs. This is mediated by endothelial cell-focal adhesion kinase (FAK), which up-regulates E-selectin, leading to preferential homing of metastatic cancer cells to these foci. Suppression of endothelial-FAK or E-selectin activity attenuates the number of cancer cells homing to these foci. Thus, localized activation of endothelial FAK and E-selectin in the lung vasculature mediates the initial homing of metastatic cancer cells to specific foci in the lungs.

metastasis | permeability

According to the widely accepted "seed and soil" hypothesis, metastatic cancer cells (the "seeds") home to and form metastases at a distant site if it provides a hospitable "soil" (1, 2). The lung is a common site for metastatic disease (3, 4). Recent reports have shown the lung "soil" may be "prepared" by distant primary tumors before metastatic cancer cell arrival. Although the role of various molecular players in this process is not resolved, this process occurs through microenvironmental changes in the lung in response to factors secreted by the primary tumors during a so-called "premetastatic" phase (5–13). "Premetastatic" events are presumed to affect the lung in a diffuse fashion, as all pulmonary microvessels are exposed to factors and cells originating from the primary tumor (14, 15). However, spontaneous lung metastasis often presents as a discrete series of lesions separated by large areas of unaffected lung tissue (16, 17). The molecular mechanisms of the formation of these focal lesions are not clear.

To identify the factors that mediate metastatic cancer cell homing to distinct areas of the lung, we used mouse models and genetic approaches to answer three questions. Can we recapitulate experimentally the heterogeneity of "premetastatic" lung "activation" by tumors, such as changes in vascular permeability previously seen with toxins (18, 19)? Does this heterogeneity have any impact on metastatic cancer cell homing? What are the pathways that mediate lung endothelial cell activation and the preferential metastatic cancer cell homing to these sites, and how?

Results

Distant Tumors Induce Focal Hyperpermeability in the "Premetastatic" Lungs, and This Effect Can Be Reproduced by Infusion of Tumor-Secreted Factors. To investigate the effects of primary tumors on the normal lungs, we grew tumors endowed with a well-characterized metastatic potential (E0771 mammary carcinoma and LLC lung carcinoma) in syngeneic C57BL/6 mice. Once tumors reached ≈6 mm in diameter, we infused Evans Blue (EB) i.v. and then excised and examined the lungs 3 h later. We found increased EB leakage in the lungs of tumor-bearing mice, with distinct, focal regions of macroscopically detectable hyperpermeability (Fig. 1*A*). To rule out the possibility that focal EB leakage was a consequence of metastatic cancer cell seeding to the lungs but rather is a direct effect of secreted factors from primary tumors, we repeated the experiments using a previously established experimental model (6, 10). We infused i.v. tumor-conditioned medium (TCM) from E0771 (ETCM) or LLC (LTCM) in non–tumor-bearing mice and examined the lungs immediately after the injection. Both ETCM and LTCM induced pulmonary vascular hyperpermeability (Fig. 1*B*) with discrete areas of EB leakage. Using ELISA, we found that LTCM/ETCM contained high concentrations of VEGF and placental growth factor (PlGF) in contrast to non-tumor cell conditioned media (NTCM). These factors are known to increase vascular permeability through direct and indirect mechanisms, respectively (20–22). Infusion of recombinant (r) VEGF or rPlGF also induced—albeit to a lesser extent—discrete foci of hyperpermeability with focal EB leakage in the lungs (Fig. S1*A*). The increase in EB leakage peaked at 3 h after stimulation and was specific to the lungs after either i.v. or intracardiac injection of the stimulus (Fig. 1 *C* and *D*). Treatment of tumor-bearing mice with an anti-VEGF blocking antibody partially inhibited lung vascular hyperpermeability (Fig. S1*B*), confirming that VEGF modulates this effect.

Metastatic Cancer Cells Preferentially Home to Hyperpermeable Foci in Lungs. To study metastatic cancer cell colonization, we developed a three-step experimental assay system (Fig. 2*A*). First, we induced focal lung hyperpermeability by tumor implantation or i.v. infusion of TCM, rVEGF, or rPlGF in non–tumor-bearing mice. Second, we infused EB or PEG-coated microbeads systemically to detect the sites of focal lung vessel leakage. Finally, we infused i.v. fluorescence-labeled metastatic cancer cells and measured the number of cells that homed to the lungs 5 or 24 h later. In tumor-bearing mice, we found that metastatic cancer cells preferentially homed to areas of high macroscopic EB leakage compared with areas of low EB leakage (after separating them by tissue microdissection; Fig. 2*B*). Prior TCM infusion

Author contributions: S.H., D.F., D.G.D., and R.K.J. designed research; S.H. and S.G. performed research; R.K.J. contributed new reagents/analytic tools; S.H., S.G., W.S.K., Y.M., D.F., D.G.D., and R.K.J. analyzed data; and S.H., S.G., D.F., D.G.D., and R.K.J. wrote the paper.

Conflict of interest statement: R.K.J. received commercial research grants from Dyax, AstraZeneca, and MedImmune; consultant fees from AstraZeneca/MedImmune, Dyax, Astellas-Fibrogen, SynDevRx, Regeneron, Genzyme, Morphosys, and Noxxon Pharma; and a speaker honorarium from Genzyme. R.K.J. owns stock in SynDevRx. No reagents or funding from these companies was used in these studies. There is no significant financial or other competing interest in the work.

Freely available online through the PNAS open access option.

[1]Present address: Department of Pharmacology, Tokyo Women's Medical University, 8-1 Kawada, Shinjyuku-ku, Tokyo 162-8666, Japan.

[2]To whom correspondence may be addressed. E-mail: dai@steele.mgh.harvard.edu, duda@steele.mgh.harvard.edu, or jain@steele.mgh.harvard.edu.

This article contains supporting information online at www.pnas.org/lookup/suppl/doi:10.1073/pnas.1100446108/-/DCSupplemental.

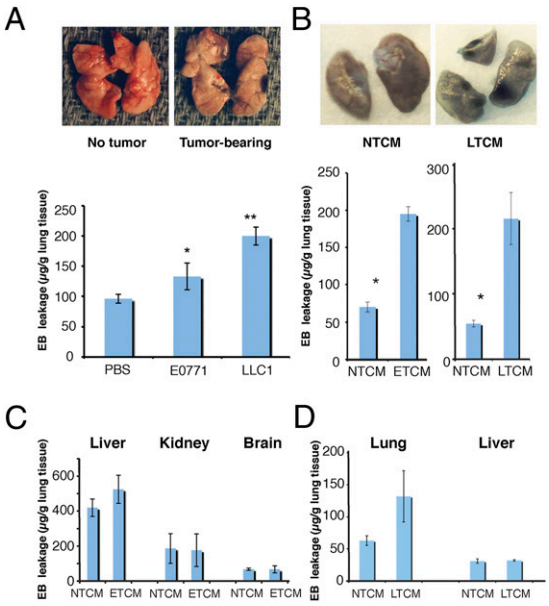

Fig. 1. Formation of hyperpermeable foci by distant tumors. (*A*) Representative images of and quantification of EB leakage in the lungs of mice bearing s.c. primary E0771 or LLC tumors, measured 3 h after EB injection. $*P < 0.05$, $**P < 0.01$ vs. s.c. PBS injection, $n = 4$–6. (*B*) Representative images of EB leakage into lungs of healthy mice 3 h after stimulation with LTCM or NTCM. LTCM and ETCM significantly increased EB leakage; $*P < 0.05$ vs. NTCM, $n = 6$. (*C*) Total EB leakage in the liver, kidney, and brain of healthy mice after stimulation by tail vein injection of NTCM or ETCM ($n = 6$). (*D*) Total EB leakage in the lung and liver of healthy mice after stimulation by intracardiac injection of NTCM vs. LTCM. $*P < 0.05$, $n = 4$. Error bars are SEM.

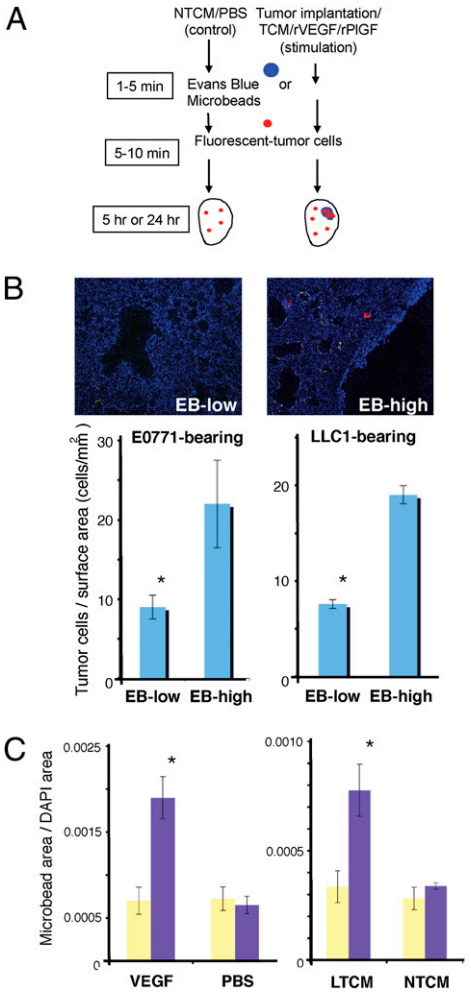

Fig. 2. Preferential homing of circulating cancer cells to regions of hyperpermeability in the lungs. (*A*) Schematic of a three-step, acute assay system to quantify metastatic cancer cell homing to different regions in stimulated lungs. (*B*) Representative images and quantification of i.v. injected metastatic cancer cells homed to areas of high vs. low EB leakage in the lungs of healthy mice stimulated by ETCM or LTCM measured 5 h after injection. $n = 6$, $*P < 0.05$. (*C*) Quantitation of microbead density (pixel/pixel) in microscopic fields surrounding metastatic cancer cells vs. paired microscopic fields with no tumor cells in the lungs of healthy mice stimulated by LTCM, NTCM, rVEGF, or PBS. $*P < 0.05$; *y*-axis scale is in multiples of 10^{-3}; $n = 16$. Error bars are SEM.

also significantly increased the total number of fluorescent cancer cells homing to the lungs of healthy mice after both 5 and 24 h, and the cells localized preferentially in hyperpermeable areas (Fig. S2 *A*–*C*). Finally, prior anti-VEGF antibody treatment significantly reduced the number of cancer cells homing to the lungs (Fig. S2*D*).

To investigate the association of cancer cells with the permeable vessels, we injected PEG-coated microbeads (instead of EB) after the induction of focal hyperpermeability by TCM or rVEGF infusion and followed by the infusion of metastatic cancer cells. We found a higher density of extravasated PEG microbeads in microscopic fields containing metastatic cancer cells (Fig. 2*C*). Of interest, microbead density was uniformly increased over a distance of 200 μm from cancer cells, before decreasing abruptly (Fig. S2*E*). This suggested that cell homing to the normal lung occurred over a region of hyperpermeability rather than a specific site of leakiness (i.e., a preexisting gap between endothelial cells within a vessel). Of note, infiltrated cancer cells in the TCM-stimulated lungs appeared larger and had a more irregular shape compared with those in healthy lungs (Fig. S2 *F* and *G*). In this model, metastatic cancer cells homed selectively to the lungs, and homing to other organs was negligible regardless of whether the cells were infused via the tail or portal vein (Fig. S2*H*).

Endothelial Focal Adhesion Kinase (FAK) Mediates Focal Lung Vessel Hyperpermeability and Metastatic Cancer Cell Homing. Because VEGF can activate the Src–FAK complex in lung endothelial cells, we next determined whether FAK activity is instigated before the arrival of cancer cells in the lungs. We found increased levels of phosphorylated FAK protein (pFAK) in areas of TCM-induced hyperpermeability (Fig. 3*A*). The expression of pFAK in lung tissue was largely colocalized with MECA-32 expression, an endothelial cell marker (Fig. S3 *A* and *B*). To determine whether endothelial cell FAK mediates the formation of hyperpermeable foci and subsequent cancer cell homing, we developed a transgenic mouse model conditionally overexpressing FRNK—the dominant negative form of FAK (23)—in endothelial cells under the control of a tetracycline response element (*tTA-FRNK* mouse; *Materials and Methods*). FRNK expression level was higher than endogenous FAK expression in the lung tissue (Fig. S3*C*) and was reduced in a time-dependent fashion after administration of doxycycline (Dox) (Fig. S3 *D* and *E*). Endothelial-specific FRNK overexpression significantly reduced the formation of hyperpermeable foci in the lungs after ETCM infusion and LTCM infusion compared with control nontransgenic mice (Fig. 3 *B* and *C*). We confirmed this finding by comparing EB leakage in *tTA-FRNK* mice at time points 0, 24, and 48 h after i.p. administration of Dox (Fig. S3*F*). Moreover, endothelial cell FRNK overexpression resulted in a significant decrease in the homing of infused metastatic cancer cells to the lungs, both of healthy mice stimulated by TCM (Fig. 3*D* and Fig.

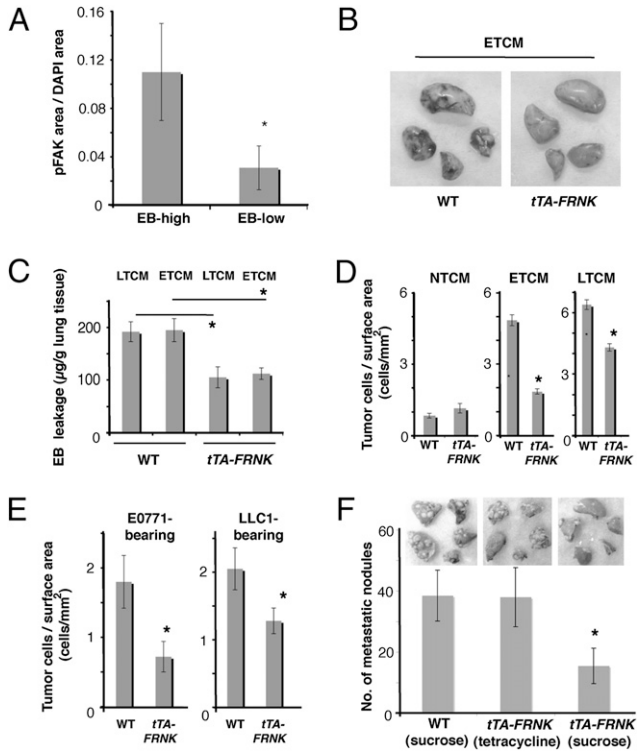

Fig. 3. Specific blockade of endothelial cell FAK activity reduces regional hyperpermeability, metastatic cancer cell homing, and the formation of macroscopic metastases. (*A*) Staining for pFAK (Y397) normalized by tissue area (pixel/pixel) in EB-high vs. EB-low leakage regions 3 h after stimulation by ETCM in wild-type mice, as measured by immunohistochemistry. $*P < 0.05$, $n = 4$. (*B*) Macroscopic distribution of EB leakage in the lungs of wild-type and *tTA-FRNK* (endothelial cell-specific) mice after stimulation with i.v. injection of ETCM. (*C*) Quantification of EB leakage in the lungs stimulated with i.v. injection of ETCM or LTCM (measured 3.5 h after EB injection). $*P < 0.05$, $n = 6$. (*D*) Metastatic cancer cell homing to the lungs of wild-type and *tTA-FRNK* mice after stimulation with i.v. injection of NTCM, ETCM, or LTCM. $*P < 0.05$, $n = 6$. (*E*) Metastatic cancer cell homing to the lungs of tumor-bearing wild-type and *tTA-FRNK* mice after stimulation with i.v. TCM, measured 48 h after i.v. injection of metastatic cancer cells. $*P < 0.05$, $n = 5$. (*F*) Number of macroscopic lung metastases in the lungs of WT mice and *tTA-FRNK* mice (either with tetracycline/sucrose drinking water or sucrose control) 3 wk after i.v. injection of LTCM and LLC cells. $*P < 0.05$, $n = 4$. Error bars are SEM.

S3*G*) and in primary tumor-bearing mice, as measured 48 h after metastatic cancer cell infusion (Fig. 3*E*). Importantly, the total macroscopic metastatic burden in the lungs was also significantly reduced 3 wk after i.v. TCM and metastatic cancer cell infusion in *tTA-FRNK* mice (Fig. 3*F*). Collectively, these data show that blocking lung endothelial cell-FAK activity reduces not only formation of discrete foci of vascular permeability but also metastatic tumor cell homing.

Lung Endothelial Cells in Hyperpermeable Foci Overexpress E-selectin. We next evaluated the microenvironmental changes within the hyperpermeable foci that might mediate the increase in metastatic cancer cell homing. Quantification of the number of myeloid ($CD11b^+$) cells in areas of high vs. low EB leakage showed no significant difference in inflammatory cell infiltration at 3.5 h after TCM injection (Fig. S4*A*). We next performed PCR array analysis to assess whether the adhesive properties of the local endothelium were altered in areas of hyperpermeability. To this end, we extracted RNA from microdissected tissue from leaky vs. nonleaky areas—induced by TCM injection in healthy wild-type mice—and measured gene expression of a panel of endothelial adhesion molecules. We found only modest changes (e.g., *E-selectin* gene showed a 1.7-fold increase after rVEGF and ≈1.4-fold after TCM stimulation). However, measurement of E-selectin protein in lung endothelial cells by immunofluorescence microscopy showed a significant increase in E-selectin expression in the hyperpermeable areas (Fig. 4*A*). Moreover, E-selectin expression after TCM stimulation was significantly reduced in the lung tissue of tTA-FRNK mice compared with wild-type mice (Fig. 4*B*). Collectively, these data suggest that endothelial cell-FAK activity mediates E-selectin expression in the hyperpermeable area.

E-selectin in Lung Endothelial Cells Mediates Metastatic Cell Homing to Hyperpermeable Foci. We next performed in vivo assays to determine the role of E-selectin in metastatic cancer cell homing to hyperpermeable foci. Immunohistochemistry revealed colocalization of pFAK and E-selectin in endothelial cells adjacent to metastatic cancer cells in the lungs of wild-type mice after TCM and cancer cell injection (Fig. S4*B*). Tumor cell homing to lungs after TCM stimulation was significantly reduced by treatment with anti–E-selectin blocking antibody in wild-type mice as well as in *E-selectin*$^{-/-}$ mice (Fig. 4*C* and Fig. S4*C*). Consistent with the observed reduction of E-selectin expression and tumor cell homing after knockdown of endothelial cell FAK function, no significant further change was seen in *tTA-FRNK* mice by E-selectin blockade (Fig. 4*C*). To further dissect the relative contribution of FAK and E-selection in the induction of hyperpermeable foci and tumor cell homing, we examined hyperpermeable lesions and cancer cell homing in the lungs of *E-selectin*$^{-/-}$ mice (24) after TCM stimulation and EB injection. Although macroscopically detectable regions of vascular hyperpermeability persisted despite the *E-selectin* deficiency, we found a reduction in metastatic cancer cell homing to the lungs of *E-selectin*$^{-/-}$ mice at both 5 and 24 h after metastatic cancer cell injection (Fig. 4 *D* and *E*). This reduction was specific for areas of hyperpermeability (Fig. 4*D*). Importantly, a reduction in cancer cell homing to the lungs was also observed in *E-selectin*$^{-/-}$ mice bearing primary tumors (Fig. 4*F*).

FAK Activation Directly Induces E-selectin Expression in Lung Endothelial Cells. To confirm that endothelial cell FAK directly regulates E-selectin expression (i.e., not via induction of local plasma leakage and inflammation), we isolated primary lung endothelial cells from wild-type and *tTA-FRNK* mice and exposed them to rVEGF in vitro. As expected, VEGF stimulation significantly increased E-selectin expression in wild-type endothelial cells (25) but not in *tTA-FRNK* endothelial cells (Fig. 5 *A* and *B*). Thus, E-selectin expression in lung endothelial cells can be induced by VEGF via FAK activation. Next, we evaluated the role of E-selectin induction by FAK in metastatic cancer cell–endothelial cell adhesion in an in vitro cancer cell adhesion assay (26). rVEGF stimulation increased the number of fluorescently labeled metastatic cancer cells attached to lung endothelial cells (Fig. 5 *C* and *D*). Addition of neutralizing anti-mouse E-selectin antibodies abolished the tumor cell adhesion to the endothelial cells (Fig. 5*D*). Conversely, rVEGF failed to induce cancer cell adhesion to the lung endothelial cells from *tTA-FRNK* mice, and anti–E-selectin blocking antibody has no effect in this setting. This indicates that FAK-induced E-selectin mediates cancer cell adhesion to lung endothelium (Fig. 5*D*).

Discussion

Lung tissue can be "activated" before the arrival of metastatic tumor cells by activation of the resident endothelial cells and macrophages by distant primary tumors in the "pre-metastatic phase" (5). Several reports have converged toward the idea of a "preparation" of the metastatic soil. Despite these reports, the precise role of various molecular and cellular factors as facilitators of nascent metastases remains controversial (12, 13). Furthermore, the presence of the candidate molecules throughout

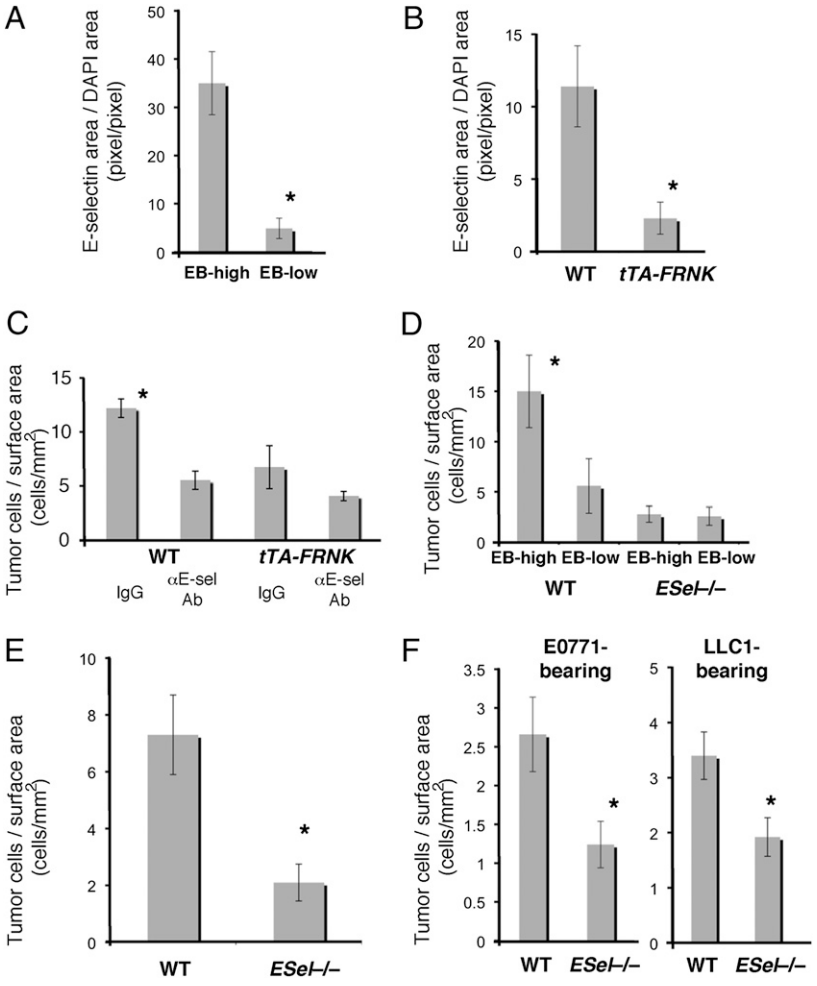

Fig. 4. E-selectin is up-regulated by endothelial FAK activation in hyperpermeable areas and mediates metastatic cancer cell homing in vivo. (*A*) E-selectin expression in areas of high vs. low EB leakage in wild-type mice stimulated with i.v. ETCM (as measured by immunohistochemistry). $*P < 0.05$, $n = 4$. (*B*) E-selectin expression in wild-type vs. *tTA-FRNK* mice stimulated with i.v. ETCM. $*P < 0.05$, $n = 4$. (*C*) In vivo assay of tumor cell homing to ETCM-stimulated lungs of wild-type and *tTA-FRNK* mice, with or without administration of an E-selectin blocking antibody. $*P < 0.05$, $n = 3$–4. (*D*) Number of metastatic cancer cells homing to areas of high vs. low EB leakage in the lungs of wild-type and *E-selectin*$^{-/-}$ mice 5 h after stimulation with i.v. ETCM. $*P < 0.05$, $n = 4$. (*E*) Metastatic cancer cell homing to the lungs of age- and sex-matched C57BL/6 (wild-type) and *E-selectin*$^{-/-}$ mice 24 h after stimulation with i.v. ETCM. $*P < 0.05$, $n = 4$. (*F*) Metastatic cancer cell homing to the lungs of tumor-bearing wild-type and *E-selectin*$^{-/-}$ mice measured 48 h after TCM and tumor cell injection. $*P < 0.05$, $n = 4$. Error bars are SEM.

the lung parenchyma does not explain the localized nature of metastatic disease.

The phenomenon of focal response of lung vasculature to stimuli (such as increased permeability after exposure to toxins) has been reported for decades (18, 19). However, the exact molecular mechanisms responsible for this heterogeneity remain elusive. Multiple secreted factors—often overexpressed in tumors (e.g., VEGF, TGF-β, TNF-α, and angiopoietin-2)—can promote vascular permeability in the lungs (5–11). VEGF released from lung metastasizing cancer cells can activate the Src-FAK complex in lung endothelial cells and promote vascular hyperpermeability, up-regulation of endothelial adhesion molecules, and cancer cell homing (27, 28). Here we demonstrate that metastatic primary tumors and soluble factors released by them can induce distinct macroscopic regions of FAK-dependent vascular hyperpermeability in the lungs.

Endothelial cell E-selectin is traditionally associated with the homing of leukocytes through rolling and tethering (29–32), and its expression is rapidly induced in response to inflammatory stimuli, such as TNF-α (peaking at 2–6 h) (33). It has previously been noted that VEGF overexpression can lead to an E-selectin-dependent increase in leukocyte rolling (34), that exposure of cultured endothelial cells to tumor-secreted factors increases E-selectin expression (25), and that VEGF directly induces E-selectin expression in endothelial cells (35). Finally, tumor cell engagement with the lung endothelium is mediated in part by E-selectin (33, 36). Here we show that lung regions that serve as discrete, fertile fields of premetastatic "soil" demonstrate an increased tumor cell homing facilitated by E-selectin up-regulation in endothelial cells via FAK.

In summary, we demonstrate that VEGF and other factors derived from primary tumors can set in motion molecular and physiological changes in distant organs before the homing of metastatic cancer cells. We show that circulating metastatic cancer cells localize preferentially in regions of vascular hyperpermeability via endothelial FAK/E-selectin mediated homing. These findings and further understanding of the cascade of pathophysiological changes in the "pre-metastatic" stroma and the molecular determinants of the metastatic cell colonization may impact strategies for preventing or controlling lung metastasis.

Materials and Methods

Reagents. Human rVEGF was supplied by NCI Research Resources. Mouse PlGF was purchased from R&D Systems. Dox, tetracycline hydrochloride, and EB were from Sigma-Aldrich and fluorescein-labeled tomato lectin ws from Vector Laboratories.

Metastatic Cancer Cell Lines and TCM. The C57BL/6 mouse-syngeneic LLC1 cell line was purchased from ATCC. The E0771 breast cancer cell line was originally established by Dr. Sirotnak (Memorial Sloan-Kettering Cancer Center, New York) and kindly provided by Dr. Mihich (Roswell Park Memorial Institute, Buffalo, NY) (37). To obtain TCM, cell lines were incubated overnight in serum-free media (DMEM, ATCC). We measured mouse VEGF and PlGF levels using the ELISA (*SI Materials and Methods*).

Animals and Tumor Models. All animal procedures were performed following the guidelines of Public Health Service Policy on Humane Care of Laboratory Animals and approved by the Institutional Animal Care and Use Committee.

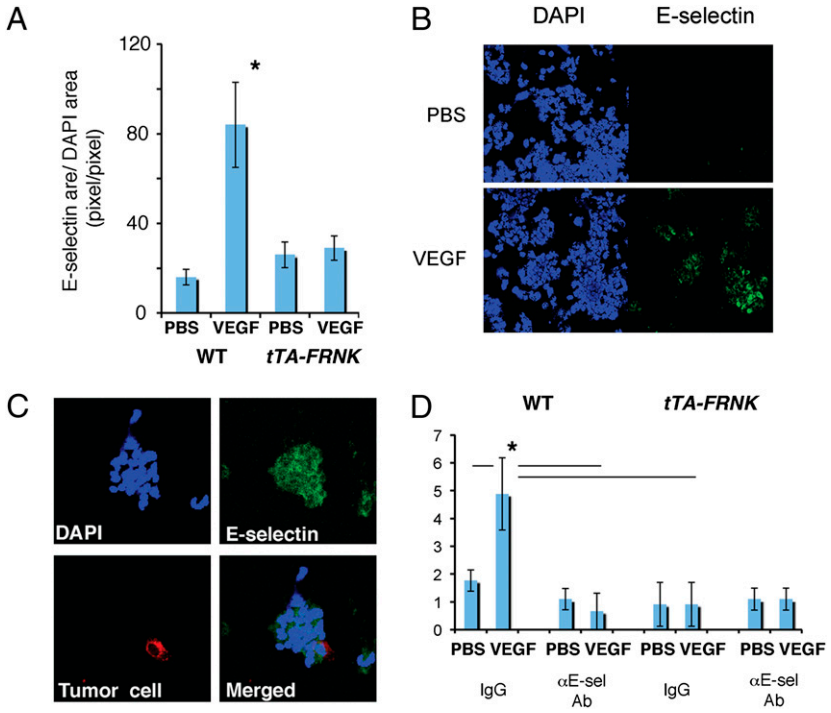

Fig. 5. Increased tumor cell adhesion to lung endothelial cells is mediated by E-selectin expression stimulated by FAK in vitro. (*A*) E-selectin expression on wild-type and *tTA-FRNK* primary lung endothelial cells after stimulation by PBS or rVEGF. $*P < 0.05$, $n = 10$. (*B*) Immunohistochemical detection of E-selectin expression in primary lung endothelial cells isolated from wild-type mice after 4 h of stimulation with 100 ng/mL rVEGF or PBS. (*C*) Representative images of rhodamine-labeled E0771 tumor cells (red) adherent to lung endothelial cells (blue), stained for E-selectin (green), in an in vitro tumor cell–endothelial cell adhesion assay. (*D*) In vitro assay of tumor cell adhesion to VEGF-stimulated primary lung endothelial cells in wild-type and *tTA-FRNK* mice. Data are shown as number of E0771 cells adhering to endothelial cells after incubation with or without anti–E-selectin blocking antibody. $*P < 0.05$, $n = 3$. Error bars are SEM.

Syngeneic tumor grafts were generated by s.c. implantation of 5×10^6 LLC1 or E0771 cells in 8- to 12-wk-old C57BL/6 mice (Jackson Labs). For tumor cell homing assays, 1–4 $\times$ 10^4 rhodamine-labeled metastatic cells were infused via tail vein. We used inducible overexpression of FRNK because, whereas endothelial-specific *FAK*$^{-/-}$ mice are embryonically lethal, in inducible endothelial-specific *FAK*$^{-/-}$ mice there is normal embryogenesis and modulation of vascular permeability in response to VEGF after FAK inhibition (38–40). For transgenic mouse experiments, we used 7- to 8-wk old tTA-VE-Cadherin promoter-driven FRNK and their wild-type littermates. *E-selectin*$^{-/-}$ mice (#008236, B6.129S4-Sele^{tm1Dmil}/J) were purchased from Jackson Labs. Age- and sex-matched C57BL/6 mice were used as controls, because the *E-selectin*$^{-/-}$ mice were back-crossed on C57BL/6 strain for 12 generations.

PEGylation of Microbeads. Forty-nanometer fluorospheres (Invitrogen) were incubated with PEG-diamine (Fluka) in polylink coupling buffer. Next, we added PolyLink EDAC (Carbodiimide) and after 2 h quenched the reaction with glycine. The resulting solution was dialyzed against PBS, and bead aggregates were removed before use.

Vascular Permeability/Leakage Assays. Assays for lung vascular permeability were performed once tumors reached ≈6 mm in diameter using i.v. infusion of EB or PEG microbeads via tail vein (20 mg/mL). In separate experiments, TCM (200–300 μL) was injected i.v. followed by EB (20 mg/mL) or PEG microbeads 1–5 min later. NTCM (200–300 μL) was used as a control. For intracardiac injection, TCM was injected directly into the left cardiac ventricle. Finally, 200 μL of rVEGF or rPlGF (100 ng/mL to 1 μg/mL) was infused i.v., followed by EB or PEG microbead infusion 1–5 min later. Gene and protein expression levels in EB-high and EB-low areas (after i.v. LTCM and rVEGF infusion) were measured using PCR array and Western blotting (*SI Materials and Methods*).

Quantification of EB Leakage. EB leakage was quantified at 3.5–5 h after infusion, as previously described (41). In brief, the pulmonary microvasculature was first flushed with PBS under physiologic pressure. The lungs were then excised, rinsed in PBS, and snap-frozen in liquid nitrogen. Frozen tissue was later homogenized in PBS and incubated in formamide at 60 °C for 16 h. To determine EB concentrations, we recorded supernatant absorbance at 620 (A_{620}) and 740 nm (A_{740}). Tissue EB content (μg EB/g lung) was calculated by correcting A_{620} for the presence of heme pigments:

$$A_{620}\ (\text{corrected}) = A_{620} - (1.426 \times A_{740} + 0.030)$$

and comparing this value to a standard curve of EB in formamide/PBS.

Cancer Cell Labeling and in Vivo Homing Assays. E0771 and LLC cells were fluorescently labeled with the PKH26 staining kit (Zynaxis), and then 2×10^4 labeled cells were infused i.v. In mice with primary tumors, the labeled cells were infused when the tumor reached 6 mm in diameter. In mice with no tumors, labeled cells were infused i.v. 6–15 min after TCM infusion. Lungs were perfused with PBS under physiologic pressure to eliminate any circulating tumor cells and then excised at 5 or 24 h after cancer cell infusion. Three randomly selected lung tissue fragments (3 mm in diameter) were selected, and two 50-μM sections per fragment were examined using confocal microscopy. Labeled cancer cell counts were normalized for total tissue surface area.

Quantitative Analysis of Extravasated Microbeads. Analysis of immunostained images was performed using in-house algorithms in Matlab software (Mathworks). Bead density was quantified by digitizing the beads using user-defined thresholds and measuring the fraction of lung tissue area covered by beads (pixels). Spatial analysis of the location of PEG microbeads relative to metastatic cancer cells was performed by measuring the bead density at specific distances from the closest cancer cell (using a 2D map).

Construction of Plasmids and Generation of Transgenic Mouse. The mouse FRNK expression vector (23), a 1.1-kb FRNK coding region corresponding to amino acids 691–1053 of mouse FAK, was kindly provided by Dr. R. Lee (Harvard Medical School, Boston). We modified the −3 upstream ATG nucleotide of FRNK from C to A and inserted it into a pTRE-Tight vector (Clontech). Transgene DNA for pronuclear injection was excised as an ApaL1 fragment. The linearized construct was injected into fertilized oocytes of DBA2 $\times$ C57BL6 (DBF_1) mice, and the eggs were implanted into pseudo-pregnant foster mothers. The offspring (F_0) were tested for chromosomal

integration of transgene by PCR. For genotyping, The PCR primers used were as follows (5′ to 3′): AAGCCTCCGAAGAGCTTGGGCT (forward) and AATCCTCCACACTGGGCTGCC (reverse). Then these mice were mated with *VE-Cadherin-tTA* mice (42). Our *tTA-FRNK* mice did not show embryonic lethality. To rapidly regulate the FRNK expression in vivo, 2 mg of Dox was administered via i.p. injection (43). Littermates were used as controls for all experiments using *tTA-FRNK* mice.

Immunofluorescence. For immunostaining of lung frozen tissue sections or dissociated lung cell suspensions, we used rat anti-mouse E-selectin (BD Pharmingen), rabbit anti-mouse FAK (pY397; Invitrogen), or mouse anti-pFAK (Tyr397, Mab 1144; Upstate), rat anti-mouse MECA32 (BD Pharmingen), and rat anti-mouse Mac1/CD11b (Serotec) antibodies. Cy3- or Cy5-conjugated secondary antibodies were used for the detection of signals by confocal microscopy. Slides were counterstained by DAPI nuclear staining.

E-selectin Antibody Blockade in Vivo. Blocking monoclonal antibodies against E-selectin (10E9.6) or control rat IgG2aκ antibodies (both from BD Pharmingen) were infused i.v. at a dose of 4 mg/kg 30 min before metastatic cancer cell infusion.

Anti-VEGF Antibody Experiments. Neutralizing anti-VEGF antibodies (R&D Systems) was incubated with TCM for 30 min before systemic infusion. In experiments using tumor-bearing mice, 10 μg of anti-VEGF antibody was infused 30 min before cancer cell infusion.

Metastatic Cancer Cell–Endothelial Cell Adhesion Assay. Lung endothelial cells were obtained using enzymatic digestion and magnetic immuno-separation (*SI Materials and Methods*). We modified a previously described protocol (26). The mouse lung endothelial cells were stimulated for 4 h with 100 ng/mL of rVEGF, then washed twice and incubated with either anti–E-selectin antibody (40 mg/mL) or control IgG. After 30 min, rhodamine-labeled E0771 cells were added at a tumor/endothelial cell ratio of 1:1. After 45 min, wells were washed to remove unattached tumor cells, the culture slide plates were fixed by PFA and counterstained by DAPI, and attached tumor cells were counted using a confocal microscope.

Data Analysis. All data are expressed mean ± SEM. Student's *t* test was used for all analyses except the microbead analyses, which used multivariate analysis of variance followed by post hoc between-groups hypothesis testing (SYSTAT 12; SYSTAT Soft) when involving multiple comparisons. We considered a p value of <0.05 to be statistically significant.

ACKNOWLEDGMENTS. We thank B. Seed and I. Garkavstev for helpful comments; L. Benjamin for providing *VE-cadherin-tTA* mice; R. Lee for providing the FRNK vector; L. Wu for help with transgenic mice; M. Dawson, P. Huang, M. Lee, C. Smith, and K. Kinzel for help in performing these experiments; and M. Ancukiewicz for statistical analysis. This study was supported by National Institutes of Health Grants R01-CA085140, R01-CA115767, P01-CA080124, R01-CA126642, and Federal Share/National Cancer Institute Proton Beam Program Income (to R.K.J.), and R01-CA096915 (to D.F.). S.H. is supported by The Scholarship Fund to Study Abroad, Japan. S.G. is supported by a Fulbright Postgraduate Award and an American Society of Clinical Oncology Young Investigator Award. W.S.K. is the recipient of a Susan G. Komen Postdoctoral Research Fellowship. R.K.J. is the recipient of the Department of Defence Breast Cancer Research Innovator Award W81XWH-10-1-0016.

1. Paget S (1889) The distribution of secondary growths in cancer of the breast. *Lancet* 1: 571–573.
2. Fidler IJ (2003) The pathogenesis of cancer metastasis: The 'seed and soil' hypothesis revisited. *Nat Rev Cancer* 3:453–458.
3. Gupta GP, et al. (2007) Mediators of vascular remodelling co-opted for sequential steps in lung metastasis. *Nature* 446:765–770.
4. Talmadge JE, Fidler IJ (2010) AACR centennial series: The biology of cancer metastasis: Historical perspective. *Cancer Res* 70:5649–5669.
5. Hiratsuka S, et al. (2002) MMP9 induction by vascular endothelial growth factor receptor-1 is involved in lung-specific metastasis. *Cancer Cell* 2:289–300.
6. Kaplan RN, et al. (2005) VEGFR1-positive haematopoietic bone marrow progenitors initiate the pre-metastatic niche. *Nature* 438:820–827.
7. Hiratsuka S, Watanabe A, Aburatani H, Maru Y (2006) Tumour-mediated upregulation of chemoattractants and recruitment of myeloid cells predetermines lung metastasis. *Nat Cell Biol* 8:1369–1375.
8. Hiratsuka S, et al. (2008) The S100A8-serum amyloid A3-TLR4 paracrine cascade establishes a pre-metastatic phase. *Nat Cell Biol* 10:1349–1355.
9. Huang Y, et al. (2009) Pulmonary vascular destabilization in the premetastatic phase facilitates lung metastasis. *Cancer Res* 69:7529–7537.
10. Kim S, et al. (2009) Carcinoma-produced factors activate myeloid cells through TLR2 to stimulate metastasis. *Nature* 457:102–106.
11. Erler JT, et al. (2009) Hypoxia-induced lysyl oxidase is a critical mediator of bone marrow cell recruitment to form the premetastatic niche. *Cancer Cell* 15:35–44.
12. Dawson MR, Duda DG, Fukumura D, Jain RK (2009) VEGFR1-activity-independent metastasis formation. *Nature*, 461: E4.
13. Dawson MR, Duda DG, Chae SS, Fukumura D, Jain RK (2009) VEGFR1 activity modulates myeloid cell infiltration in growing lung metastases but is not required for spontaneous metastasis formation. *PLoS ONE* 4:e6525.
14. Riethdorf S, Pantel K (2008) Disseminated tumor cells in bone marrow and circulating tumor cells in blood of breast cancer patients: Current state of detection and characterization. *Pathobiology* 75:140–148.
15. Mostert B, Sleijfer S, Foekens JA, Gratama JW (2009) Circulating tumor cells (CTCs): Detection methods and their clinical relevance in breast cancer. *Cancer Treat Rev* 35: 463–474.
16. Schlappack OK, Baur M, Steger G, Dittrich C, Moser K (1988) The clinical course of lung metastases from breast cancer. *Klin Wochenschr* 66:790–795.
17. Jaklitsch MT, et al. (2001) Sequential thoracic metastasectomy prolongs survival by re-establishing local control within the chest. *J Thorac Cardiovasc Surg* 121:657–667.
18. Pietra GG, Szidon JP, Carpenter HA, Fishman AP (1974) Bronchial venular leakage during endotoxin shock. *Am J Pathol* 77:387–406.
19. Gerbino AJ, Glenny RW (2002) Lung albumin accumulation is spatially heterogeneous but not correlated with regional pulmonary perfusion. *J Appl Physiol* 92:279–287.
20. Ferrara N, Gerber HP, LeCouter J (2003) The biology of VEGF and its receptors. *Nat Med* 9:669–676.
21. Nagy JA, Benjamin L, Zeng H, Dvorak AM, Dvorak HF (2008) Vascular permeability, vascular hyperpermeability and angiogenesis. *Angiogenesis* 11:109–119.
22. Fischer C, Mazzone M, Jonckx B, Carmeliet P (2008) FLT1 and its ligands VEGFB and PlGF: Drug targets for anti-angiogenic therapy? *Nat Rev Cancer* 8:942–956.
23. Hakuno D, Takahashi T, Lammerding J, Lee RT (2005) Focal adhesion kinase signaling regulates cardiogenesis of embryonic stem cells. *J Biol Chem* 280:39534–39544.
24. Milstone DS, et al. (1998) Mice lacking E-selectin show normal numbers of rolling leukocytes but reduced leukocyte stable arrest on cytokine-activated microvascular endothelium. *Microcirculation* 5:153–171.
25. Melder RJ, et al. (1996) During angiogenesis, vascular endothelial growth factor and basic fibroblast growth factor regulate natural killer cell adhesion to tumor endothelium. *Nat Med* 2:992–997.
26. Russell J, et al. (2000) Regulation of E-selectin expression in postischemic intestinal microvasculature. *Am J Physiol Gastrointest Liver Physiol* 278:G878–G885.
27. Eliceiri BP, et al. (2002) Src-mediated coupling of focal adhesion kinase to integrin alpha(v)beta5 in vascular endothelial growth factor signaling. *J Cell Biol* 157:149–160.
28. Kim MP, Park SI, Kopetz S, Gallick GE (2009) Src family kinases as mediators of endothelial permeability: Effects on inflammation and metastasis. *Cell Tissue Res* 335: 249–259.
29. Bevilacqua MP, Stengelin S, Gimbrone MA, Jr., Seed B (1989) Endothelial leukocyte adhesion molecule 1: An inducible receptor for neutrophils related to complement regulatory proteins and lectins. *Science* 243:1160–1165.
30. Springer TA (1994) Traffic signals for lymphocyte recirculation and leukocyte emigration: The multistep paradigm. *Cell* 76:301–314.
31. Hynes RO, Wagner DD (1996) Genetic manipulation of vascular adhesion molecules in mice. *J Clin Invest* 98:2193–2195.
32. Jain RK, et al. (1996) Leukocyte-endothelial adhesion and angiogenesis in tumors. *Cancer Metastasis Rev* 15:195–204.
33. Barthel SR, Gavino JD, Descheny L, Dimitroff CJ (2007) Targeting selectins and selectin ligands in inflammation and cancer. *Expert Opin Ther Targets* 11:1473–1491.
34. Detmar M, et al. (1998) Increased microvascular density and enhanced leukocyte rolling and adhesion in the skin of VEGF transgenic mice. *J Invest Dermatol* 111:1–6.
35. Tabatabai G, et al. (2008) VEGF-dependent induction of CD62E on endothelial cells mediates glioma tropism of adult haematopoietic progenitor cells. *Brain* 131: 2579–2595.
36. Köhler S, Ullrich S, Richter U, Schumacher U (2010) E-/P-selectins and colon carcinoma metastasis: First in vivo evidence for their crucial role in a clinically relevant model of spontaneous metastasis formation in the lung. *Br J Cancer* 102:602–609.
37. Ewens A, Mihich E, Ehrke MJ (2005) Distant metastasis from subcutaneously grown E0771 medullary breast adenocarcinoma. *Anticancer Res* 25(6B):3905–3915.
38. Weis SM, et al. (2008) Compensatory role for Pyk2 during angiogenesis in adult mice lacking endothelial cell FAK. *J Cell Biol* 181:43–50.
39. Shen TL, et al. (2005) Conditional knockout of focal adhesion kinase in endothelial cells reveals its role in angiogenesis and vascular development in late embryogenesis. *J Cell Biol* 169:941–952.
40. Braren R, et al. (2006) Endothelial FAK is essential for vascular network stability, cell survival, and lamellipodial formation. *J Cell Biol* 172:151–162.
41. Wang F, et al. (2002) Role of inducible nitric oxide synthase in pulmonary microvascular protein leak in murine sepsis. *Am J Respir Crit Care Med* 165:1634–1639.
42. Sun JF, et al. (2005) Microvascular patterning is controlled by fine-tuning the Akt signal. *Proc Natl Acad Sci USA* 102:128–133.
43. Schönig K, Schwenk F, Rajewsky K, Bujard H (2002) Stringent doxycycline dependent control of CRE recombinase in vivo. *Nucleic Acids Res* 30:e134.